THE ASTROPHYSICAL JOURNAL, 454:683–687, 1995 December 1

EVIDENCE FOR AN OBSCURED QUASAR IN THE GIANT RADIO GALAXY PKS 0634 – 205

CHRIS SIMPSON[1]
Space Telescope Science Institute, 3700 San Martin Drive, Baltimore, MD 21218
M. J. WARD
Astrophysics, Oxford University, Keble Road, Oxford OX1 3RH, UK
AND
A. S. WILSON[2]
Space Telescope Science Institute, 3700 San Martin Drive, Baltimore, MD 21218
Received 1995 April 12; accepted 1995 June 7

ABSTRACT

We report on optical and near-infrared imaging and spectroscopy of the giant radio galaxy PKS 0634–205. The images longward of 2 μm reveal the presence of an extremely red compact source coincident with the nucleus, which is not detected at shorter wavelengths. The observed $K-L$ color of this source, the [O III] λ5007 flux and the soft X-ray flux, are consistent with the spectral energy distribution of a typical quasar observed through a visual extinction $A_V \sim 30$ magnitudes. Our 2 μm spectrum shows strong narrow Paα, but has insufficient sensitivity and wavelength coverage to reveal broad Paα from the putative quasar at the predicted level.

Subject headings: galaxies: individual (PKS 0634–205) — infrared: galaxies — quasars: general

1. INTRODUCTION

In the unified scheme for extragalactic radio sources (Scheuer 1987; Barthel 1989), radio-loud quasars and powerful (i.e., Fanaroff-Riley class II; Fanaroff & Riley 1974) radio galaxies are intrinsically the same class of object, with their observed differences being caused by orientation effects. A prediction of this model is that the nonstellar continuum and broad permitted lines observed in quasars are still present in the spectra of radio galaxies, but are heavily obscured along our line of sight. Although some objects possess a scattering region that reflects this radiation toward us so that it can be seen at optical wavelengths (e.g., 3C 234, Antonucci 1984), in others the quasar spectrum can only be seen by observing at wavelengths where the obscuration is lower, e.g., hard X-ray and near-infrared wavelengths. Such observations allow an estimate of the nuclear reddening to be made (for Cygnus A see Arnaud et al. 1987; Djorgovski et al. 1991; Ueno et al. 1994).

PKS 0634–205 is a giant radio galaxy with an overall projected linear extent $\sim$1.2 Mpc (Danziger, Goss, & Frater 1978, hereafter D78; we assume $H_0 = 50$ km s^{-1} Mpc^{-1} and $q_0 = 0$ throughout this paper), which was identified by Bolton, Clarke, & Ekers (1965) as an isolated elliptical at a redshift of $z = 0.056$ (Searle & Bolton 1968). Based on its radio structure and power ($P_{1415\,\mathrm{MHz}} = 10^{26}$ W Hz^{-1}; D78), PKS 0634–205 is classified as an FR II radio source, and would therefore be expected to harbor a quasar nucleus, whose signature may be observable at infrared and X-ray wavelengths.

In this paper, we present optical, infrared, and X-ray data for PKS 0634–205. Our *Kn* and *L* images reveal a compact nuclear source that we suggest is the transmitted continuum of a quasar seen through approximately 30 visual magnitudes of dust extinction. This hypothesis is supported by the other data in our multiwavelength analysis.

2. IMAGING

Near-infrared images of PKS 0634–205 were taken on the night of 1993 February 2 through the *J* and *Kn* filters[3] using IRIS (Allen 1992) on the 3.9 m Anglo-Australian Telescope (AAT) with a pixel size of 0.″61. The galaxy was observed at five different locations on the array to remove the effects of bad pixels, and an equal length of time was spent observing nearby regions of sky. After correcting for the nonlinear gain of the array, the bias level and dark current, the frames were divided by a flat field produced from observations of a tungsten lamp. The sky frames were then median filtered and subtracted from the individual object exposures, and the resultant frames were registered and combined by median filtering. A more detailed description of the data reduction, including photometric calibration, will be given in a future paper, which will present images of a further 13 radio galaxies observed during the run. There was a total on-source integration time of 300 s at *J* and 900 s at *Kn*. Conditions were photometric throughout and the seeing was about 1″.

In addition, an image was taken on 1994 January 18 at *L* (3.42 μm) with IRCAM2 on the 3.9 m United Kingdom Infrared Telescope (UKIRT). The pixel size was 0.″62 and the seeing approximately 1.″2. The observations employed standard infrared "jittering" techniques (see, e.g., Dunlop & Peacock 1993), with the source being observed in nine different locations in a 3×3 grid with points separated by 8″. Photometric calibration was performed using the standard star HD 44612.

Optical ($BVR_c I_c$) images of PKS 0634–205 were taken on the night of 1993 April 20 on the South African Astronomical Observatory 1.0 m telescope, using an RCA CCD with 0.″78 pixels in $\sim$2″ seeing. Each exposure was 900 s. The bias level was subtracted from each image and flat-fielding was performed using observations of the twilight sky.

[1] Previously at Astrophysics Department, Oxford University.
[2] Also Astronomy Department, University of Maryland.

[3] The *Kn* filter is very similar to the *K'* filter (Wainscoat & Cowie 1992), with an effective wavelength of 2.10 μm and a magnitude zero point of about 710 Jy.

The full set of optical and infrared images is presented in Figure 1. We note that the surface brightness becomes more sharply peaked near the nucleus at longer wavelengths, signifying redder colors in the center of the galaxy. Although such an effect can be caused by dust reddening or stellar population gradients, we will argue that in this case it results from the presence of a compact nuclear source at the longer wavelengths.

3. SPECTROSCOPY

An optical spectrum covering the wavelength range 4050 Å–1 μm was taken on the night of 1992 April 10 with the AAT, and was reduced as described in Simpson et al. (1993). A 2″ wide slit was used in ~1.″9 seeing at a position angle of 122° (i.e., in the approximate direction of the central bar of the "Z" shaped extended emission-line structure; see Hansen, Nørgaard-Nielsen, & Jørgensen 1987, hereafter H87) and the nuclear spectrum was obtained by binning approximately 4″ along the slit.

We find that the overall spectral shape is very similar to that seen by D78. However, we find a significantly lower ratio of Hα + [N II]/H$\beta \approx 8.3$ (we cannot deblend the lines since our resolution is only 20 Å), as compared to the values of 12.4 and 13.6 obtained by D78 and Storchi-Bergmann, Mulchaey, & Wilson (1995), respectively, through smaller apertures. Comparing our line fluxes with those obtained by these authors, we suggest that there may be a compact region of higher reddening coincident with the nucleus that dominates the spectra obtained by both these groups, whereas our larger aperture observations suggest an extinction estimate more applicable to the extended nuclear emission-line region.

We present the optical spectrum, corrected for a Galactic extinction of $A_V = 1.2$ mag in Figure 2. The apparent absence of the Mg I absorption feature (which is prominent in D78's spectrum) reflects its location at the join between the two spectra; the flux calibration is uncertain over the wavelength range affected by the dichroic.

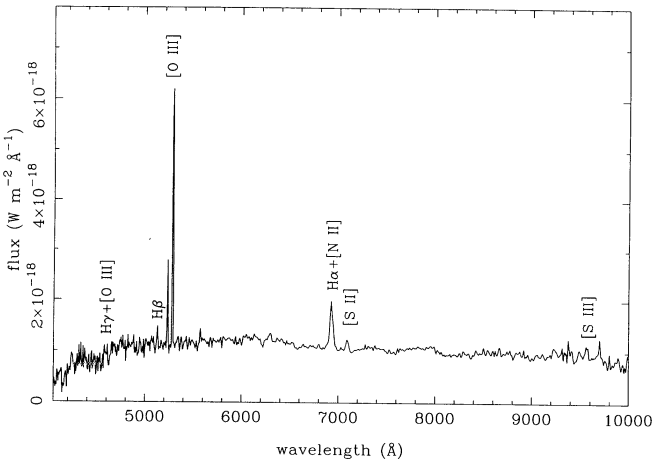

FIG. 2.—Optical spectrum of PKS 0634−205, after correction for A_V(Gal) = 1.2 mag using the reddening law of Howarth (1983). Two spectrographs were used—the resolution of the blue arm ($\lambda \lesssim 5500$ Å) was 2.5 Å and the resolution of the red arm was 20 Å. The spectrum has been smoothed with a 10 Å boxcar, and the major emission lines are labeled.

A 2 μm spectrum of PKS 0634−205 was obtained on the night of 1994 January 9 using the CGS4 spectrometer on UKIRT. The same position angle was used as for the optical spectrum, although the slit width was 3″ and the seeing was ~1″. Both the galaxy and the standard star (BS 1983, $K = 2.42$) were observed at two positions along the slit, separated by 30″ to facilitate sky subtraction. Atmospheric features were removed by assuming that BS 1983's intrinsic spectrum could be approximated by a 6350 K blackbody, and the residual "seeing ripple" after flux calibration was removed in the standard manner. The spectrum was extracted over 3″—

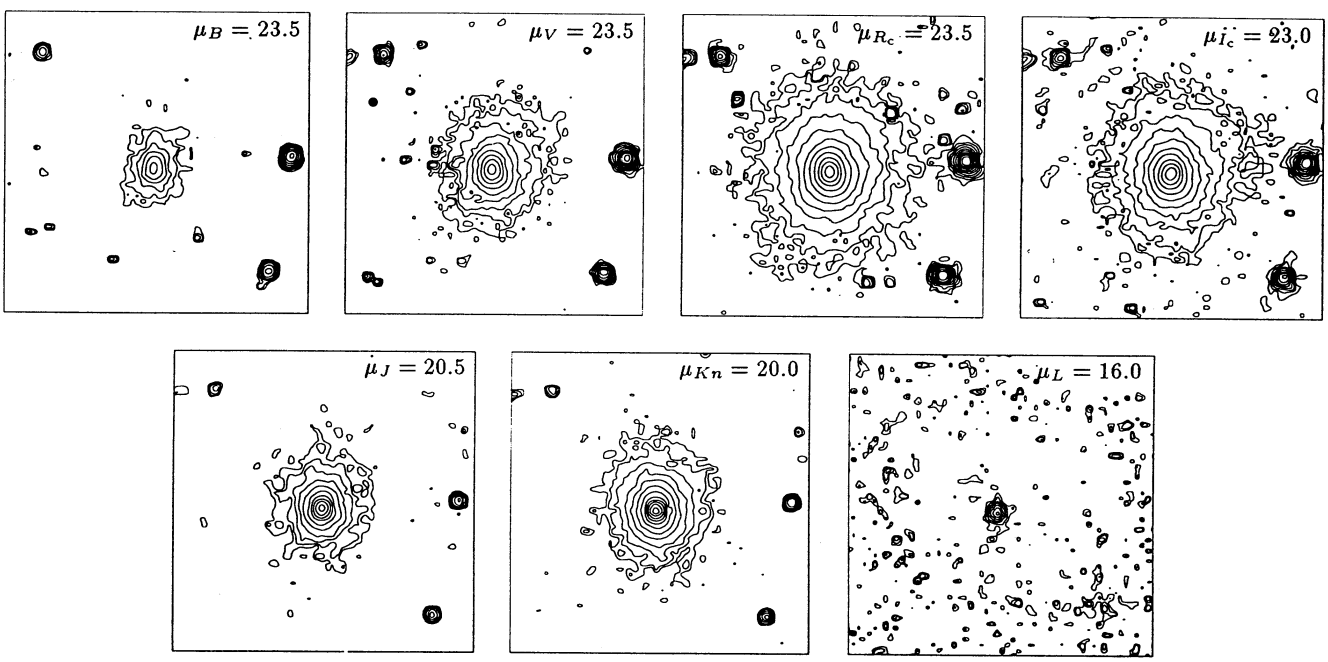

FIG. 1.—BVR_cI_c, J, Kn, and L images of PKS 0634−205. North is up, and east is to the left. Each image is approximately 45″ × 45″, and contour levels are at intervals of 0.5 mag. The value of the lowest contour (in mag arcsec^{-2} at zero air mass) is shown in the top right of each frame. The noise increases toward the edges of the L band frame because these regions of sky were observed for a shorter time than the central region.

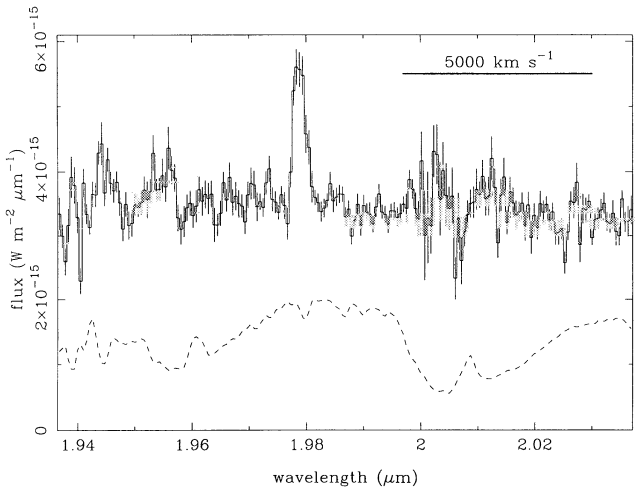

FIG. 3.—Flux calibrated CGS4 spectrum of PKS 0634−205, after correction for Galactic reddening. The narrow Paα line is clearly detected. The dashed line shows the relative atmospheric transmission.

there was no noticeable line emission beyond this region—and is presented in Figure 3. The atmospheric absorption features varied in strength independently during the course of the integration, and hence could not be fully removed from the final spectrum.

We first note that the continuum level, when extrapolated to 2.1 μm, corresponds to $Kn = 12.91$, in excellent agreement with that derived from the IRIS image of Figure 1. Second, the flux of the narrow Paα line is found to be $(5.5 \pm 0.5) \times 10^{-18}$ W m^{-2} (after correction for Galactic reddening), so the flux ratio Paα/Hβ ≈ 0.81 ± 0.15 [after correction for Galactic reddening using the reddening law of Howarth 1983; we measure an Hβ flux of $(1.8 \pm 0.3) \times 10^{-18}$ W m^{-2}], greatly in excess of the case B value (0.28), and suggestive of reddening intrinsic to the radio galaxy. However, relatively more Hβ line flux was lost due to the smaller slit width and worse seeing for the optical observations. We attempt to correct for these differences by modeling the central emission-line region as an elliptical Gaussian with major axis FWHM = 2″ at PA = 50° (estimated from H87) and negligible width in the perpendicular direction. Convolving this model with the seeing and determining the flux within our slit (assuming the slit was centered on the emission-line peak), we find that ∼60% more emission was included in the infrared than in the optical aperture. The corrected flux ratio is therefore Paα/Hβ ≈ 0.5, which implies 0.6 magnitudes of visual extinction at the source, in addition to the extinction in the Milky Way. All future reddening corrections will include $A_V = 1.2$ mag (Galactic) and $A_V = 0.6$ mag (PKS 0634−205) for a total of $A_V = 1.8$ mag (uncertain by ∼0.2 mag). While this value is lower than that derived from the Hα/Hβ decrement in the spectra of D78 and Storchi-Bergmann et al. (1995), for the reason suggested earlier, it is consistent with the Balmer decrement in our spectrum if we attempt to separate the Hα and [N II] lines by using the ratio between these lines given by D78 and Storchi-Bergmann et al. (1995).

4. THE NUCLEAR CONTINUUM SOURCE

4.1. *Separation of Stellar and Nonstellar Components*

In order to use the infrared data to infer the nuclear obscuration, it is first necessary to separate the stellar and nonstellar light. As discussed in Simpson (1994), the only satisfactory way to do this is by modeling the surface brightness distribution of the galaxy. The radial surface brightness profile was constructed for each of the seven broadband images by fitting a sequence of elliptical isophotes whose semimajor axes were at one pixel intervals. We used the IRAF "ellipse" task and continued fitting outward until the signal-to-noise ratio was less than 2. The radial surface brightness profile was then fitted with a de Vaucouleurs $r^{1/4}$ spheroid plus an unresolved nuclear source, both convolved with a Gaussian profile to represent the effects of seeing. An iterative quasi-Newton algorithm was used to minimize the value of the χ^2 statistic. The results are summarized in Table 1. As fitting procedures such as this are sensitive to the assumed value of the seeing, we allowed it to vary as a free parameter, but in all cases the best-fit value of the seeing was within 10% of the FWHM of stellar images on the frames. The exception was the *L*-band image, for which the seeing was fixed at the value determined from the standard star image, to ensure that the fit was sufficiently well constrained.

Our ability to fit all the optical profiles successfully with a de Vaucouleurs law suggests there is little patchy extinction. The nuclear source seen at the *Kn* and *L* bands must, therefore, either be absent at shorter wavelengths or obscured by dust with a spatial extent much less than the seeing. Because the unresolved source dominates the starlight in the central regions of the galaxy at *L* band, our estimate of the nuclear magnitude is rather insensitive to the parameters used to describe the spheroid. Thus, although the *L* band fit to the spheroid is poorly constrained and the effective radius is undoubtedly too large (one expects to see a decline in effective radius as one observes at longer wavelengths since the central regions of early-type galaxies are generally redder than the outer regions; see, e.g., Penereiro et al. 1994) the effect on our estimate of the nuclear magnitude is at a level of less than 20%. We place an uncertainty of 0.15 mag on both of our nuclear detections. It is important to note that, although the nonstellar source dominates at the center of the *L* band image, it contributes only ∼40% of the flux within a 5″ aperture. The remainder comes from the starlight, the $Kn - L$ color of which is consistent with that of a giant elliptical. We favor an interpretation of the nuclear source as the transmitted continuum of a quasar seen through a large optical depth of foreground material, in line with the unification models of Scheuer (1987) and Barthel (1989).

TABLE 1

RESULTS OF THE FITS TO THE RADIAL SURFACE BRIGHTNESS PROFILES OF PKS 0634−205

Filter	m_n	μ_s	r_e	χ^2/ν	Σ_n
B	...	16.54	14.74	1.1/8	...
V	...	14.52	8.40	9.3/14	...
R_c	...	13.35	7.49	3.6/17	...
I_c	...	13.41	8.23	7.1/17	...
J	...	11.14	5.15	0.8/10	...
Kn	16.53	9.63	4.25	4.6/14	5.6
L	12.90	9.37	6.02	0.8/2	14.5

NOTES.—The magnitude of the nuclear source, m_n, central surface brightness, μ_s (in mag arcsec^{-2}), and effective radius (in arcsec) of the spheroid, the quality of fit (minimum value of the χ^2 statistic and number of degrees of freedom), and the statistical significance of detection of the nucleus, Σ_n, are listed. Note that m_n and μ_s represent observed magnitudes at zero air mass, and have not been corrected for reddening.

4.2. *The Extinction to the Nuclear Source*

4.2.1. *Infrared Color*

The simplest, and least model-dependent, way to estimate the nuclear reddening is by comparing the observed color of the nucleus with that seen in unreddened low-redshift quasars. From Neugebauer et al. (1987), the near-infrared spectral index for these objects is $\alpha = -1.2 \pm 0.3$, corresponding to an intrinsic color $Kn - L = 1.70 \pm 0.16$, and a color excess for PKS 0634−205 of $E(Kn - L) = 1.93 \pm 0.27$ (Table 1). Using the reddening law of Howarth (1983), we find that $A_V = 13.7E(Kn - L)$, and hence $A_V = 26.5 \pm 3.7$ mag (including the Galactic reddening).

4.2.2. *Equivalent Width of the* [O III] λ5007 Line

Since the equivalent width of the [O III] λ5007 line is observed to lie within a fairly narrow range in low-redshift quasars (Miller et al. 1992), presumably because its emission is dominated by direct nuclear photoionization, we can use the flux of this line to infer the flux density of the unobscured optical quasar continuum. Such a method has already been successfully applied to IC 5063 (Simpson, Ward, & Kotilainen 1994). In that paper, we used the total [O III] flux, as the extent of the [O III] emission in IC 5063 is small enough to be unresolved at the distances of the quasars for which the [O III] equivalent width relationship was derived. That is clearly not the case for the much larger (~70 kpc, H87) extended emission-line region of PKS 0634−205; indeed, it is unclear whether all the extranuclear line emission in PKS 0634−205 is photoionized by the nucleus (see Lacy & Rawlings 1994). Although we prefer to derive the unobscured continuum flux density from the nuclear [O III] λ5007 alone, we also perform the calculations using the total line flux (from H87, which we correct only for Galactic reddening).

Due to the light loss occasioned by the finite slit width in our spectroscopic observations, we use the line flux reported by H87 and correct it for the total reddening of $A_V = 1.8$ mag determined above. We obtain a reddening-corrected [O III] line flux of 8.9×10^{-17} W m^{-2}, (2.1×10^{-16} W m^{-2} if we use the total line flux), which implies an unobscured visual magnitude of $V \approx 15$ ($V \approx 14$). Since the optical–near-infrared continuum of a quasar is well-described by a power-law away from the 1 μm minimum, we can use our observed $Kn - L$ color and inferred optical continuum level to solve for the nuclear reddening and optical–infrared spectral index. This is not independent of the method used in the previous section, but we allow the spectral index to vary as a free parameter, and introduce the unobscured nuclear continuum level (as inferred from the [O III] line flux) as an additional constraint. Figure 4 represents this procedure graphically, and we obtain values of $A_V = 32.5 \pm 2.5$ (35.3 ± 2.5) and $\alpha = -0.46 \pm 0.34$ ($\alpha = -0.06 \pm 0.33$; $S_\nu \propto \nu^\alpha$). This spectral index is consistent (at the 2 σ level) with that of low-redshift quasars.

4.2.3. *Soft X-Ray Flux*

PKS 0634−205 was observed with the *Einstein* Imaging Proportional Counter (IPC) on 1980 March 22. A "source" is marginally detected at the position of the radio galaxy; extraction by the standard "Local Detect" algorithm (Harris et al. 1990) reveals its formal significance to be 2.3 σ, at a level of $(2.5 \pm 1.1) \times 10^{-3}$ counts s^{-1}.

We can make a crude estimate of the nuclear reddening from this observation. We first extrapolate our inferred optical continuum to 1 μm assuming a standard quasar SED, and estimate the 2 keV X-ray flux using the relationship between infrared and X-ray luminosity for low-redshift quasars (Kriss 1988). We assume an X-ray spectral index $\alpha = -0.7$ (see, e.g., Pounds et al. 1990; Lawson et al. 1992) and determine what range of column densities, N_H, will produce count rates in the *Einstein* IPC consistent with the observations. For a normal gas-to-dust ratio, $A_V = 5 \times 10^{-22} N_H$, and we estimate $A_V = 37^{+126}_{-8}$. This is clearly consistent with the values derived above, but also with much greater columns. It is also important to note that the observed X-ray luminosity in the IPC passband is only a factor of ~2 greater than has been observed for some "normal" galaxies of comparable optical luminosity, and thus, a significant fraction of the observed emission may not come from the obscured active nucleus. Clearly, a direct measurement of a low-energy cutoff from an X-ray spectrum is necessary to provide a tighter consistency check on the results from our optical–near-infrared analysis. We shall present the results from an analysis of *ASCA* data at a later date.

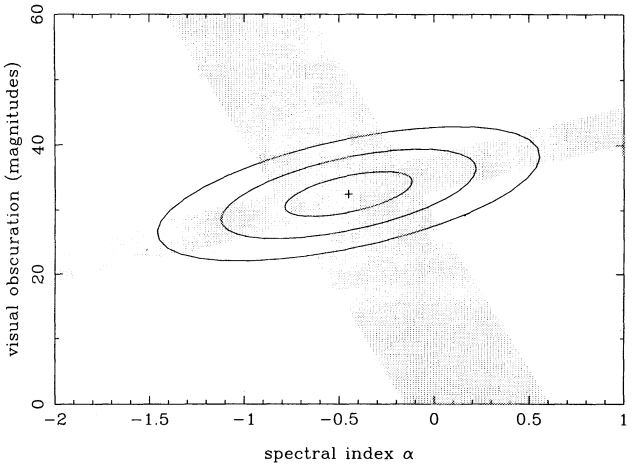

FIG. 4.—Allowed parameter space for the visual obscuration and spectral index ($S_\nu \propto \nu^\alpha$) of the quasar nucleus in PKS 0634−205. The shaded region running from bottom left to top right of the figure represents the range of values allowed by the 1 σ uncertainty in the observed nuclear $Kn - L$ color. The other shaded region shows the parameter space consistent with the (inferred, unobscured) continuum at $\lambda_{rest} = 5007$ Å and the (observed, obscured) L band continuum. The ellipses enclose the regions acceptable at the 1, 2, and 3 σ confidence levels.

5. DETECTABILITY OF BROAD PASCHEN α

In addition to a high-quality X-ray spectrum, the detection of broad wings to the near-infrared hydrogen recombination lines would also serve to tighten our extinction estimate and prove beyond doubt the existence of a quasar nucleus. Using the tight relation between [O III] λ5007 and broad Hβ flux for quasars (Miller et al. 1992), we can predict the unobscured fluxes of the broad hydrogen lines. Assuming case B recombination, we expect the flux of unobscured Paα to be

$$f_{Pa\alpha} = 7.9^{+5.1}_{-3.1} \times 10^{-17} \text{ W m}^{-2} .$$

Applying the extinction estimate derived above, we therefore expect to observe a ratio of broad to narrow-line flux of ~50%. Our CGS4 spectrum has insufficient wavelength coverage, and is affected too strongly by atmospheric features, to allow a useful upper limit to be placed on the observed broad line flux.

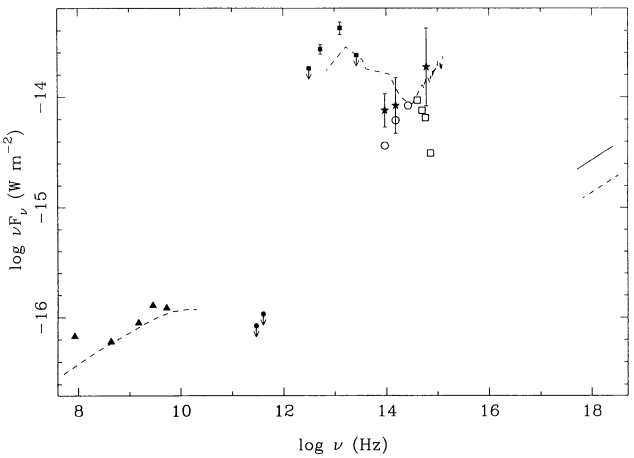

FIG. 5.—Spectral energy distributions of PKS 0634−205 and 3C 351. Solid symbols represent the SED of the active nucleus in PKS 0634−205: triangles are radio data for the entire source, circles are upper limits from the JCMT (Hughes & Ward 1994), squares are the rereduced *IRAS* data, stars show the inferred, unobscured optical–near-infrared continuum, and the solid diagonal line is the 2–10 keV continuum level, after correction for the inferred photoelectric absorption. The open symbols show the aperture photometry of the galaxy within a 3″ aperture (with no correction for obscuration): circles for the near-infrared *JKnL* fluxes, and squares for the $BVR_c I_c$ measurements. Superposed (*dashed lines*) is the SED of 3C 351, a "typical" steep-spectrum RLQ; radio data are from Kühr et al. (1981), optical and infrared data from Neugebauer et al. (1987), and 2 keV X-ray flux from Tananbaum et al. (1986).

6. SPECTRAL ENERGY DISTRIBUTION

In the course of our multiwavelength analysis of PKS 0634−205, we retrieved and rereduced the *IRAS* scans of the region. We find that the source is strongly detected at both 25 and 60 μm, and marginally detected at 100 μm. However, due to the cirrus confusion at this last wavelength (the radio galaxy is at relatively low Galactic latitude, $b \approx 12°$), we choose to place an upper limit of 570 mJy on the 100 μm flux. No detection was made at 12 μm. We present a full spectral energy distribution of PKS 0634−205 in Figure 5, together with that of 3C 351, which Neugebauer et al. (1987) use as a typical radio-loud quasar. The bolometric luminosity of the quasar in PKS 0634−205 is inferred to be $\sim 2 \times 10^{38}$ W. We note that the absolute near-infrared magnitudes of the host galaxy ($M_{Kn} = -26.2$, calculated by integrating our model of the spheroid out to large radius) and the unobscured nucleus ($M_{Kn} = -24.6$) lie on the correlation found by Kotilainen & Ward (1994) between these two quantities for the Seyfert 1's and quasars in the hard X-ray selected sample of Piccinotti et al. (1982).

7. CONCLUSION

We have shown the existence of a reddened source coincident with the nucleus of the giant radio galaxy PKS 0634−205. If explained by thermal dust emission, this dust must be at a temperature of $\gtrsim 1000$ K and thus requires some compact and sustained heating source. While a quasar may not be the only plausible explanation, our data are entirely consistent with the prediction of unification models that PKS 0634−205 is an obscured radio-loud quasar, with an extinction to the nucleus of $A_V = 30 \pm 4$ magnitudes.

The authors wish to express their gratitude to Dave Axon, Jeremy Bailey, Steve Eales, David Hughes, and Duncan Law-Green for obtaining the UKIRT and JCMT data presented in this paper. We also wish to thank Steve Rawlings for useful discussions. This research has made use of the NASA/IPAC extragalactic database (NED), operated by the Jet Propulsion Laboratory, Caltech, under contract with the National Aeronautics and Space Administration, and was supported in part by *HST* grant GO-3724 and NASA grant NAGW-3268. C. S. also acknowledges financial support from a PPARC studentship. The Space Telescope Science Institute is operated by AURA, Inc., under NASA contract NAS 5-26555.

REFERENCES

Allen, D. A. 1992, Anglo-Australian Observatory User Manual, UM-30 (Epping: Anglo-Australian Obs.)
Antonucci, R. R. J. 1984, ApJ, 278, 499
Arnaud, K. A., Johnstone, R. M., Fabian, A. C., Crawford, C. S., Nulsen, P. E. J., Shafer, R. A., & Mushotzky, R. F. 1987, MNRAS, 227, 241
Barthel, P. D. 1989, ApJ, 336, 606
Barvainis, R. 1987, ApJ, 320, 537
Bolton, J. G., Clarke, N. E., & Ekers, R. D. 1968, Australian J. Phys., 18, 627
Danziger, I. J., Goss, W. M., & Frater, R. H. 1978, MNRAS, 184, 341
Djorgovski, S., Weir, N., Matthews, K., & Graham, J. R. 1991, ApJ, 372, L67
Dunlop, J. S., & Peacock, J. A. 1993, MNRAS, 263, 936
Fanaroff, B. L., & Riley, J. M. 1974, MNRAS, 167, 31P
Ferland, G. J., & Osterbrock, D. E. 1986, ApJ, 300, 658
Ferland, G. J., Netzer, H., & Shields, G. A. 1979, ApJ, 232, 382
Hansen, L., Nørgaard-Nielsen, H. U., & Jørgensen, H. E. 1987, A&AS, 71, 465
Harris, D. E., et al. 1990, The *Einstein Observatory* Catalog of IPC X-Ray Sources (Cambridge: Smithsonian Inst. Astrophys. Obs.)
Howarth, I. D. 1983, MNRAS, 203, 301
Hughes, D. H., & Ward, M. J. 1994, private communication
Kotilainen, J. K., & Ward, M. J. 1994, MNRAS, 266, 953
Kriss, G. A. 1988, ApJ, 324, 809
Kühr, H., Witzel, A., Pauliny-Toth, I. I. K., & Nauber, U. 1981, A&AS, 45, 367
Lacy, M., & Rawlings, S. 1994, MNRAS, 270, 431
Lawson, A. J., Turner, M. J. L., Williams, O. R., Stewart, G. C., & Saxton, R. 1992, MNRAS, 259, 743
Miller, P., Rawlings, S., Saunders, R., & Eales, S. 1992, MNRAS, 254, 93
Neugebauer, G., Green, R. F., Matthews, K., Schmidt, M., Soifer, B. T., & Bennett, J. 1987, ApJS, 63, 615
Osterbrock D. E. 1989, Astrophysics of Gaseous Nebulae and Active Galactic Nuclei (Mill Valley: University Science Books)
Penereiro, J. C., de Carvalho, R. R., Djorgovski, S., & Thompson, D. 1994, A&AS, 108, 461
Piccinotti, G., Mushotzky, R. F., Boldt, E. A., Holt, S. S., Marshall, F. E., Serlemitsos, P. J., & Shafer, R. A. 1982, ApJ, 253, 485
Pounds, K. A., Nandra, K., Stewart, G. C., George, I. M., & Fabian, A. C. 1990, Nature, 344, 132
Scheuer, P. A. G. 1987, in Superluminal Radio Sources, ed. J. A. Zensus & T. J. Pearson (Cambridge: Cambridge Univ. Press), 104
Searle, L., & Bolton, J. G. 1968, ApJ, 154, L101
Simpson, C. 1994, MNRAS, 271, 247
Simpson, C., Clements, D. L., Rawlings, S., & Ward, M. 1993, MNRAS, 262, 889
Simpson, C., Ward, M., & Kotilainen, J. 1994, MNRAS, 271, 250
Storchi-Bergmann, T., Mulchaey, J. S., & Wilson, A. S. 1992, ApJ, 395, L73
———. 1995, private communication
Tadhunter, C., & Tsvetanov, Z. 1989, Nature, 341, 422
Tananbaum, H., Avni, Y., Green, R. F., Schmidt, M., & Zamorani, G. 1986, ApJ, 305, 57
Ueno, S., Koyama, K., Nishida, M., Yamauchi, S., & Ward, M. J. 1994, ApJ, 431, L1
Wainscoat, R. J., & Cowie, L. L. 1992, AJ, 103, 332